

Spatiotemporal Mode-Locking in Lasers with Large Modal Dispersion

Yihang Ding,^{1,‡} Xiaosheng Xiao^{1b,2,‡,*} Kewei Liu,¹ Shuzheng Fan,² Xiaoguang Zhang^{1b,2} and Changxi Yang^{1,†}

¹State Key Laboratory of Precision Measurement Technology and Instruments, Department of Precision Instruments, Tsinghua University, Beijing 100084, China

²State Key Laboratory of Information Photonics and Optical Communications, School of Electronic Engineering, Beijing University of Posts and Telecommunications, Beijing 100876, China



(Received 6 November 2019; accepted 1 February 2021; published 3 March 2021)

Dissipative nonlinear wave dynamics have been investigated extensively in mode-locked lasers with single transverse mode, whereas there are few studies related to three-dimensional nonlinear dynamics within lasers. Recently, spatiotemporal mode locking (STML) was proposed in lasers with small modal (i.e., transverse-mode) dispersion, which has been considered to be critical for achieving STML in those cavities because the small dispersion can be easily balanced. Here, we demonstrate that STML can also be achieved in multimode lasers with much larger modal dispersion, where we find that the intracavity saturable absorber plays an important role for counteracting the large modal dispersion. Furthermore, we observe a new STML phenomenon of passive nonlinear autoselection of single-mode mode locking, resulting from the interaction between spatiotemporal saturable absorption and spatial gain competition. Our work significantly broadens the design possibilities for useful STML lasers thus making them much more accessible for applications, and extends the explorable parameter space of the novel dissipative spatiotemporal nonlinear dynamics that can be achieved in these lasers.

DOI: [10.1103/PhysRevLett.126.093901](https://doi.org/10.1103/PhysRevLett.126.093901)

Mode-locked lasers based on single-mode fibers are popular platforms for studying the behavior of dissipative nonlinear wave dynamics [1], because they provide a simple way to perform nonlinear science research. Additionally, mode-locked fiber lasers are promising for many applications. However, single-mode fibers are challenged by the ever-increasing demand for higher-energy lasers, as well as for larger data capacities in the field of optical fiber communications [2,3]. The use of multimode fibers (MMFs) is the most obvious way to overcome these limitations due to the larger mode area and additional spatial degree of freedom of MMFs.

In the field of nonlinear science, a multimode optical system based on MMFs, combining both temporal and spatial characteristics, can provide a better test bed than a conventional system composed of single-mode fibers. There is great significance in studying nonlinear dynamics in three-dimensional optical systems composed of MMFs, as these dynamics are related to important issues in physics in term of spatiotemporal dynamics. The various nonlinear spatiotemporal dynamics in passive graded-index MMFs have been investigated extensively recently, including studies of spatiotemporal instability [4–6], spatial beam cleaning [7–12], supercontinuum generation [12–17], and control of nonlinear multimode interactions [18,19]. In addition, nonlinear pulse propagation in amplifiers composed of active MMFs was studied [20–23]. However, very little work on MMF cavities with multimode nonlinear dynamics has been performed.

Recently, Wright *et al.* proposed spatiotemporal mode locking (STML), i.e., both the longitudinal and transverse modes were locked simultaneously, in a cavity composed of graded-index MMFs [24], and the key factor that makes the STML possible in those MMF cavities was considered as the small modal dispersion of the graded-index MMFs. The small modal (i.e., spatial or transverse-mode) dispersion of graded-index MMFs is comparable to chromatic (i.e., longitudinal-mode) dispersion and these dispersions can be compensated for by strong intracavity spatial and spectral filtering in those cavities [24], allowing transverse modes to travel together. According to this, large modal dispersion will pose a challenge for achieving STML in MMF cavities. It is interesting to know whether and how STML can be supported in MMF cavities with large modal dispersion.

The realization of STML inside an MMF cavity relies on a delicate balance among the intracavity linear and nonlinear effects, including modal and chromatic dispersions, inter- and intramodal nonlinearities, filtering, gain and loss. The significant influence of cavity dispersion on the dissipative nonlinear dynamics has been widely observed and investigated in single-mode fiber lasers [1]. Similarly, in MMF cavities, different dispersion parameters will cause different dynamical process of self-organization and different nonlinear spatiotemporal phenomena. Therefore, if STML can be achieved in MMF cavities with large modal dispersion, a further important question is

what the dynamical process of the spatiotemporal self-organization is.

As the counterpart of the graded-index fibers, step-index fibers usually exhibit much larger (ten times) modal dispersion (i.e., walk-off among different modes) (Refs. [25,26] and Secs. S3.1 of the Supplemental Material [27]). Thus step-index MMFs can serve as an appropriate medium for our curious investigations. From an application perspective, the development of useful STML lasers are greatly limited by the rarity of graded-index multimode gain fibers, which are not commercially available, likely due to the complex distribution of the refractive index compared to that of step-index fibers. Quasi-single-mode gain fibers have been used in some cavities (Refs. [34–36] and the first cavity of Ref. [24]). Although these cavities allow for observing a variety of spatiotemporal effects (e.g., soliton molecule reported in our previous work [34]), they are severely restricted compared to full-multimode systems in terms of both the range of physics that can be observed and the potential performance of the lasers. Contrary to the rarity of active graded-index MMFs, the active step-index ones are easy to commercially obtain, despite the much larger modal dispersion.

In this Letter, we show how to realize STML by using active step-index MMFs with large modal dispersion, and report the observation of novel nonlinear spatiotemporal dynamics within the cavity. In these MMF cavities with large modal dispersion, the key to achieve STML is the effects of the intracavity saturable absorber (SA). By optimizing the lengths of MMFs, the SA plays two critical roles. One is the basic function of SA, passively modulating the cavity loss, which is usually expected, and the other is balancing the large walk off among transverse modes,

which is an additional effect achieved in this cavity. It is found that the spatiotemporal evolution of the multimode pulses is quite different from that inside the graded-index MMF cavity. Moreover, we observed an interesting nonlinear phenomenon of passive beam autoselection, i.e., the transition from multimode to single-mode mode-locking state. We found evidence for this important regime in which the fast nonlinear effects of SA interact with the spatial gain competition to lead to the passive nonlinear auto-selection of single-mode mode locking.

Numerical simulations are first conducted to analyze the spatiotemporal evolution of pulses in an MMF cavity with step-index gain fibers (detailed in Secs. S1–S3 of Ref. [27]). The cavity used in the simulations is shown in Fig. 1(a). The light is amplified through propagation in an active step-index MMF and then coupled with a segment of passive graded-index MMF and transmitted through a lumped SA. Then a spectral filter is applied, and the light is injected back into the gain fiber. The spectral filter is usually used in mode-locking fiber lasers with normal dispersion to meet the requirement of pulse self-consistency [37]. The step-index MMF is the same as that in Fig. S1, and the parameters of both MMFs are in accordance with those of the fibers used in the following experiments [27].

With appropriate cavity parameters, we found that stable STML could be achieved in the MMF laser cavity with the active step-index MMF. Typical numerical result for the STML state is presented in Figs. 1(b)–1(e) (see more in Secs. S2, S3 and movie S1 of the Supplemental Material [27]). The intercavity evolution of the output of two typical modes, modes 1 and 6, over 80 roundtrips in the cavity is shown in Fig. 1(b), starting from small pulses. The pulses

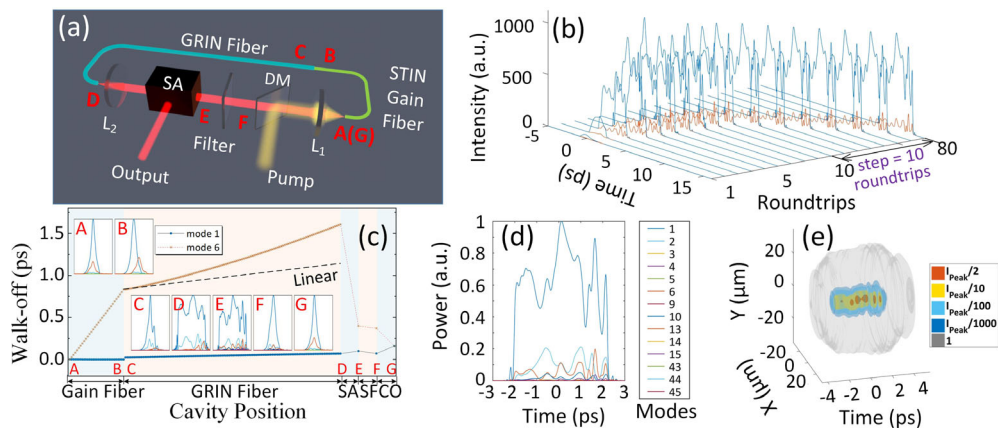


FIG. 1. Mode-resolved simulation of STML in an MMF laser with an active step-index MMF. (a) Cavity used in the simulation ($L_{1,2}$: lenses, DM: dichroic mirror). (b) Intercavity evolution of the output pulse. For clarity, only modes 1 and 6 are shown. (c) Intracavity evolution of the walk-off between modes 1 and 6 when stable STML is achieved. The data are calculated by the center of gravity for both modes relative to a reference frame moving with the linear group velocity of mode 1. Black dashed line: linear walk-off of mode 6 related to mode 1. Insets A–G: Temporal pulse shapes at different cavity positions labeled in (a) [A/B: input/output of the step-index (STIN) gain fiber, C/D: Input/output of the graded-index (GRIN) fiber, E: after SA, F: after spectral filtering (SF), G: input of the gain fiber via coupling (CO)]; The lengths of step-index and graded-index MMFs are 0.6 and 2.4 m, respectively. (d) Mode-resolved temporal output. (e) The corresponding spatiotemporal intensity of (d). I_{peak} : peak intensity of the multimode pulse.

reach a steady operation state quickly. The intracavity pulse evolution in the final round-trip is plotted in Fig. 1(c), where the walk-off between two typical modes, modes 1 and 6, is presented. The walk-off between the two modes constantly increases in the MMFs. Notably, the dramatic decrease in walk-off by SA indicates that SA plays an important role in pulling the modes together to achieve self-consistency and realizing STML in the cavity. The mode-resolved temporal output is plotted in Fig. 1(d), and Fig. 1(e) shows the corresponding spatiotemporal intensity of the output pulse. Overall, the combination effects of intracavity spatial filtering, spectral filtering and SA are strong enough to counteract the large modal dispersion. Among them, the SA takes a great proportion in balancing the dispersion, which is the key to let STML work in the MMF cavities with large modal dispersion.

Note that in the graded-index fiber, the movement speed of mode 6 is much larger than the linear velocity calculated from modal dispersion, which is indicated by the black dashed line in Fig. 1(c). This larger walk-off is induced by nonlinear multimode interactions, which is greatly affected by the large modal dispersion in step-index fiber (see details in Sec. S3.3 of Ref. [27]). Comparing Fig. 1(c) to the evolution in a similar cavity but with small modal dispersion shown in Fig. S3 [27], it shows that the large modal dispersion results in quite different evolutions.

Based on the simulations, we established an MMF laser cavity with a step-index gain fiber accordingly (see Fig. S5 in Ref. [27]). Nonlinear polarization rotation was used to establish an artificial and ultrafast SA [38]. Figure 2 records the gradual transition to STML in the MMF cavity with increasing pump power (recorded every 0.1 W). Once the pump power reaches 2.5 W, STML can be easily self-started by adjusting the pump power only. The spectra and corresponding beam profiles at different pump powers are depicted in Figs. 2(d)–2(k). As the pump power increases through the thresholds (around 2.5/3.7 W), sudden changes take place in the beam profile, as well as the temporal and spectral outputs, as the operation state transits between multimode continuous-wave lasing and mode locking, indicating that STML occurs. More proofs of STML are given in Sec. S5 of the Supplemental Material [27].

To determine which cavity can support STML, we experimentally tested many cavities with various lengths of the MMFs (see section Sec. S5.3 of Ref. [27]). In general, a long step-index fiber induces large walk-off among the transverse modes, which is difficult to compensate for. Additionally, a long passive graded-index fiber induces a strong SA effect through the accumulation of nonlinear polarization rotation, which aids in the formation of STML. Therefore, a cavity configuration with a short step-index gain fiber plus a relatively long graded-index fiber is preferred for achieving STML.

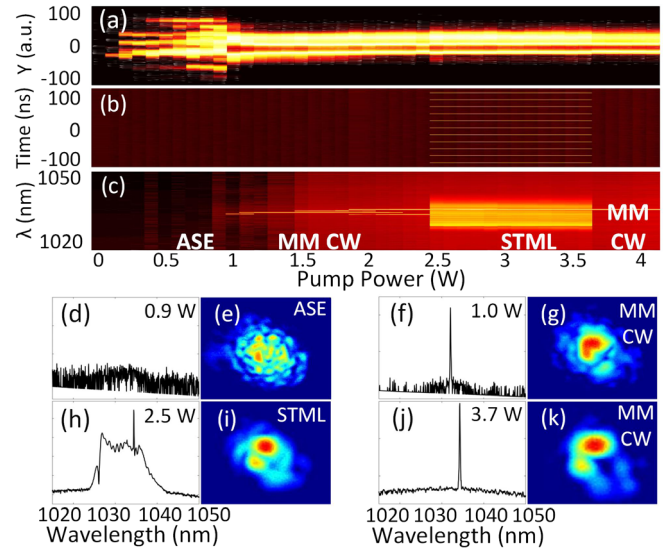


FIG. 2. Evolution of output with increasing pump power in the cavity. The evolutions of (a) the beam profile integrated over one dimension (the intensity is normalized for each step), (b) temporal output over a 200-ns span, and (c) spectrum. As the pump power increases, the field transitions from amplified spontaneous emission (ASE) [(d)–(e)] to multimode continuous-wave lasing (MM CW) [(f)–(g)] and then to STML [(h)–(i)] and eventually to MM CW [(j)–(k)]. The values of corresponding pump powers are labeled.

Furthermore, we experimentally observed a nonlinear phenomenon of beam autoselection mode locking, i.e., a multimode STML state transiting to a mode-locking state with a single transverse mode by adjusting the orientation of the intracavity wave plate only. A typical transition is given in Fig. 3. With appropriate optical coupling state, wave plate sets, pump power, etc., in the cavity, stable multimode STML is achieved. The beam profile of the output shown in Fig. 3(a) indicates that it is multimode. Then, by rotating the wave plate carefully, the multimode STML state transitions to another mode-locking state, as shown in Figs. 3(d)–3(g). Compared to the old state, the beam profile and spectrum of the new state change, while the repetition rate remains the same.

The output beam profile of the new state, measured in the near field [Fig. 3(d)], contains two symmetric lobes. By the assumption of the LP_{11} profile, one can conduct that the field can be described by a Laguerre Gauss distribution [11]. According to the mathematical properties of the Fourier transform of the Laguerre Gauss function, the far field of the LP_{11} mode is a Laguerre Gauss distribution as well. The far-field beam profile is recorded in Fig. 3(e), with a double peak, indicating that it is associated with an LP_{11} mode-locking state. To further verify the LP_{11} mode locking, the upper and lower lobes shown in Fig. 3(d) are measured separately, and the corresponding pulse trains and spectra are compared in Figs. 3(f)–3(g). The pulse trains and spectra recorded from the two lobes are almost

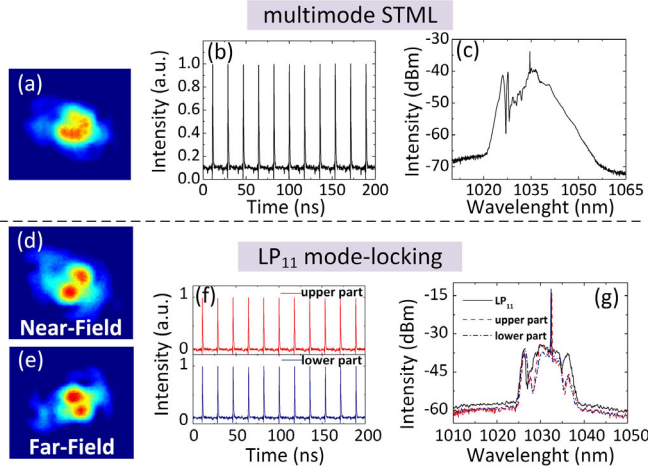


FIG. 3. Transition from multimode STML to single transverse-mode (LP_{11}) mode locking in the same MMF cavity by adjusting the intracavity waveplate only. (a) Beam profile, (b) pulse train, and (c) spectrum of the output pulse train of the multimode STML state. (d)–(g) LP_{11} mode locking. Output beam profiles in the near field (d) and far field (e). (f) Pulse trains of the upper and lower parts of the beam profile in (d). (g) Spectra of the entire beam profile and the upper and lower parts of the beam profile in (d).

the same. The spectrum of the entire beam is slightly different from those of the two lobes, likely due to the existence of a few high-order modes. We note that the occurrence of beam autoselection mode locking depends on the coupling condition from the free space to the step-index MMF. Only in a certain coupling state can the transition be achieved. Occasionally, we further observed a bistable state, i.e., the state frequently transitions between multimode and single-mode mode locking in a certain fixed cavity setup.

In an MMF cavity, both the nonlinear gain of active fiber and the nonlinear loss of SA induce nonlinear energy exchange among transverse modes. The former comes from spatial gain competition, and the latter is illustrated in Fig. S4 [27]. The SA originates from nonlinear polarization rotation in our cavity, and its parameters are adjusted by the rotation of wave plates. Therefore, the observed transition of mode-locking states can be directly attributed to the adjustment of the parameters of the SA. Subsequently, the effect of SA interacts with other effects in the cavity, especially with the spatial gain competition, determining the output mode components.

We demonstrate it by simulating the STML states in an MMF cavity with a different SA parameter, saturation power P_{sat} . Under $P_{\text{sat}} = 12$ kW (case 1), the stable STML outputs are presented in Figs. 4(a), 4(b). In this state, mode 1 dominates, and there are mainly two modes, modes 1 and 6, with large walk-off that propagate in the MMFs. In this case, the intracavity evolution of the walk-off between these two modes is similar to that in Fig. 1(c). For case 2

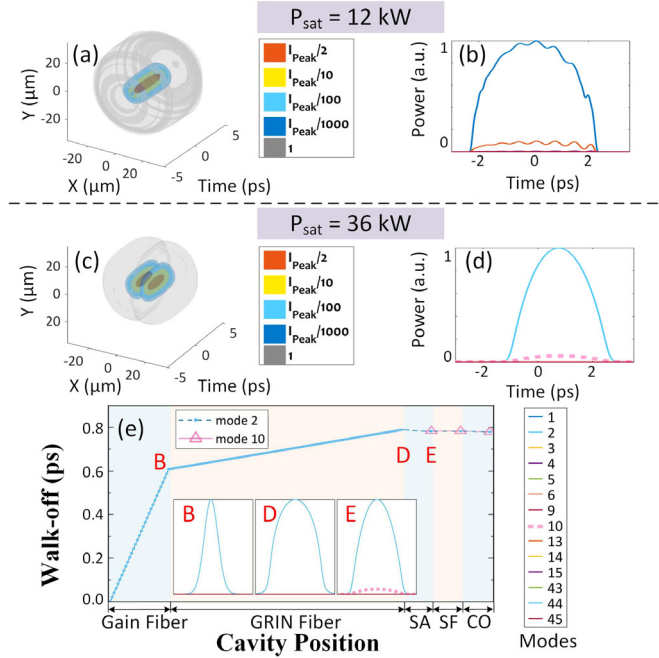


FIG. 4. Simulation of STML in an MMF laser with different SA saturation powers (P_{sat}), demonstrating the dependence of STML state on the SA parameter. (a), (c) Spatiotemporal intensity of and (b), (d) mode-resolved stable output pulses for (a)–(b) $P_{\text{sat}} = 12$ kW (case 1) and (c)–(d) $P_{\text{sat}} = 36$ kW (case 2). (e) Intracavity evolution of the walk-off of mode 2 (and mode 10 after the SA) relative to a reference frame moving with the linear group velocity of fundamental mode when stable STML is achieved in case 2. Insets B, D-E: mode-resolved temporal pulse shape at the different cavity positions labelled in Fig. 1(a) [B/D: output of the step-index gain fiber/graded-index (GRIN) fiber, E: after the SA].

with a P_{sat} value of 36 kW, the corresponding intracavity evolution and stable output are given in Figs. 4(c)–4(e) (See movie S2 [27] for a comparison of the intercavity evolutions of these two cases with the same initial input). With increasing P_{sat} , mode 2 (LP_{11}) emerges, although other conditions are fixed. In this case, there is only one transverse-mode (LP_{11}) that propagates in both the step-index and graded-index MMFs, as shown in Fig. 4(e), which is significantly different from case 1. Note that after propagation through the SA, mode 2 splits into mode 2 plus a small part of mode 10, as shown in Figs. 4(d)–4(e), likely because the profile of mode 10 resembles that of mode 2. The corresponding spatiotemporal intensity in Fig. 4(c) is dominated by the shape of the LP_{11} mode. We note that, a similar STML state transition has been predicted in a paper published after the submission of this work [39].

In conclusion, the spatiotemporal self-organization of the multimode solitons is demonstrated in MMF lasers with large modal dispersion, the nonlinear dynamical process of which is quite different from that inside the graded-index MMF cavity. Moreover, a new spatiotemporal nonlinear

dynamic, passive auto-selection of single-mode mode locking, is reported and analyzed. SA plays critical roles in achieving STML, as well as in these spatiotemporal dynamics. From another perspective, for a multimode cavity with large modal dispersion, two mode-locking states are expected. One is multimode, assisted by the SA balancing the walk-off among different transverse modes, and the other is single mode (without suffering from the modal walk-off), which is achieved through the interactions between the SA and mode competition.

The introduction of active step-index MMFs into STML cavities provides new opportunities for research at both the scientific and technological levels. From a fundamental perspective, although the nonlinear dynamic process has been extensively studied in mode-locked single-mode lasers, it is still poorly understood in multimode cavities with immense spatiotemporal complexity. Our results expand the understanding of complex nonlinear spatiotemporal dynamics. In addition, the passive nonlinear auto-selection of mode appears to allow for a compromise between the benefits of multimode and single-mode systems. Furthermore, the STML lasers with large modal dispersion extend the explorable parameter space of the new spatiotemporal dynamics that can be achieved within them. In terms of technology, our work greatly broadens the design possibilities and provides convenient architectures for STML cavities because the active step-index MMFs are easy to fabricate and are commercially available. STML lasers with step-index multimode gain fibers are promising to be exploited as convenient platforms for the investigation of high-dimensional nonlinear science and as high-power, ultrashort optical pulse sources.

The authors would like to thank Dr. Logan G. Wright for helpful discussion and suggestion, and the help of numerical simulations. This work was partially supported by the National Key Scientific Instrument and Equipment Development Project of China under Grant No. 2014YQ510403, National Natural Science Foundation of China (51527901, 61975090), Fund of State Key Laboratory of IPOC (BUPT), P. R. China (No. IPOC2019ZZ02 and IPOC2020ZT02). X. X. and Y. D. conceived the ideas. Y. D. conducted the experiments. X. X. performed the simulations. K. L., S. F., and X. X. helped performing the experiments. X. X., X. Z., and C. Y. supervised the project. Y. D. and X. X. co-wrote the manuscript. All authors commented on the manuscript.

*Corresponding author.

xsxiao@bupt.edu.cn

†Corresponding author.

cxyang@mail.tsinghua.edu.cn

*These authors contributed equally to this work.

[1] P. Grelu and N. Akhmediev, Dissipative solitons for mode-locked lasers, *Nat. Photonics* **6**, 84 (2012).

- [2] D. J. Richardson, Filling the light pipe, *Science* **330**, 327 (2010).
- [3] D. Richardson, J. Fini, and L. E. Nelson, Space-division multiplexing in optical fibres, *Nat. Photonics* **7**, 354 (2013).
- [4] L. G. Wright, Z. Liu, D. A. Nolan, M.-J. Li, D. N. Christodoulides, and F. W. Wise, Self-organized instability in graded-index multimode fibres, *Nat. Photonics* **10**, 771 (2016).
- [5] K. Krupa, A. Tonello, A. Barthélémy, V. Couderc, B. M. Shalaby, A. Bendahmane, G. Millot, and S. Wabnitz, Observation of geometric parametric instability induced by the periodic spatial self-imaging of multimode waves, *Phys. Rev. Lett.* **116**, 183901 (2016).
- [6] U. Teğin and B. Ortaç, Spatiotemporal instability of femto-second pulses in graded-index multimode fibers, *IEEE Photonics Technol. Lett.* **29**, 2195 (2017).
- [7] Z. Liu, L. G. Wright, D. N. Christodoulides, and F. W. Wise, Kerr self-cleaning of femtosecond-pulsed beams in graded-index multimode fiber, *Opt. Lett.* **41**, 3675 (2016).
- [8] K. Krupa, A. Tonello, B. M. Shalaby, M. Fabert, A. Barthélémy, G. Millot, S. Wabnitz, and V. Couderc, Spatial beam self-cleaning in multimode fibres, *Nat. Photonics* **11**, 237 (2017).
- [9] R. Guenard *et al.*, Nonlinear beam self-cleaning in a coupled cavity composite laser based on multimode fiber, *Opt. Express* **25**, 22219 (2017).
- [10] E. Deliancourt, M. Fabert, A. Tonello, K. Krupa, A. Desfarges-Berthelebot, V. Kermene, G. Millot, A. Barthélémy, S. Wabnitz, and V. Couderc, Wavefront shaping for optimized many-mode Kerr beam self-cleaning in graded-index multimode fiber, *Opt. Express* **27**, 17311 (2019).
- [11] E. Deliancourt *et al.*, Kerr beam self-cleaning on the LP 11 mode in graded-index multimode fibers, *OSA Continuum* **2**, 1089 (2019).
- [12] A. Niang *et al.*, Spatial beam self-cleaning and supercontinuum generation with Yb-doped multimode graded-index fiber taper based on accelerating self-imaging and dissipative landscape, *Opt. Express* **27**, 24018 (2019).
- [13] G. Lopez-Galmiche, Z. S. Eznavah, M. Eftekhar, J. A. Lopez, L. Wright, F. Wise, D. Christodoulides, and R. A. Correa, Visible supercontinuum generation in a graded index multimode fiber pumped at 1064 nm, *Opt. Lett.* **41**, 2553 (2016).
- [14] K. Krupa *et al.*, Spatiotemporal characterization of supercontinuum extending from the visible to the mid-infrared in a multimode graded-index optical fiber, *Opt. Lett.* **41**, 5785 (2016).
- [15] M. A. Eftekhar, L. Wright, M. Mills, M. Kolesik, R. A. Correa, F. W. Wise, and D. N. Christodoulides, Versatile supercontinuum generation in parabolic multimode optical fibers, *Opt. Express* **25**, 9078 (2017).
- [16] L. G. Wright, D. N. Christodoulides, and F. W. Wise, Controllable spatiotemporal nonlinear effects in multimode fibres, *Nat. Photonics* **9**, 306 (2015).
- [17] L. G. Wright, S. Wabnitz, D. N. Christodoulides, and F. W. Wise, Ultrabroadband dispersive radiation by spatiotemporal oscillation of multimode waves, *Phys. Rev. Lett.* **115**, 223902 (2015).
- [18] O. Tzang, A. M. Caravaca-Aguirre, K. Wagner, and R. Piestun, Adaptive wavefront shaping for controlling nonlinear

- multimode interactions in optical fibres, *Nat. Photonics* **12**, 368 (2018).
- [19] M. Eftekhar, Z. Sanjabi-Eznaveh, H. Lopez-Aviles, S. Benis, J. Antonio-Lopez, M. Kolesik, F. Wise, R. Amezcua-Correa, and D. Christodoulides, Accelerated nonlinear interactions in graded-index multimode fibers, *Nat. Commun.* **10**, 1638 (2019).
- [20] J. Nicholson, A. Desantolo, W. Kaenders, and A. Zach, Self-frequency-shifted solitons in a polarization-maintaining, very-large-mode area, Er-doped fiber amplifier, *Opt. Express* **24**, 23396 (2016).
- [21] J. Nicholson, R. Ahmad, A. DeSantolo, and Z. Várallyay, High average power, 10 GHz pulses from a very-large-mode-area, Er-doped fiber amplifier, *J. Opt. Soc. Am. B* **34**, A1 (2017).
- [22] R. Florentin, V. Kermene, J. Benoist, A. Desfarges-Berthelemot, D. Pagnoux, A. Barthélémy, and J.-P. Huignard, Shaping the light amplified in a multimode fiber, *Light-Sci. Appl.* **6**, e16208 (2017).
- [23] R. Guenard *et al.*, Kerr self-cleaning of pulsed beam in an ytterbium doped multimode fiber, *Opt. Express* **25**, 4783 (2017).
- [24] L. G. Wright, D. N. Christodoulides, and F. W. Wise, Spatiotemporal mode-locking in multimode fiber lasers, *Science* **358**, 94 (2017).
- [25] L. G. Wright, Z. M. Ziegler, P. M. Lushnikov, Z. Zhu, M. A. Eftekhar, D. N. Christodoulides, and F. W. Wise, Multimode nonlinear fiber optics: massively parallel numerical solver, tutorial, and outlook, *IEEE J. Sel. Topics Quantum Electron.* **24**, 1 (2017).
- [26] L. G. Wright, Z. M. Ziegler, P. M. L. Z. Zhu, and F. W. Wise, Advanced examples of use of the GMMNLSE solver, [Online]. Available: <https://wise.research.engineering.cornell.edu>, <https://github.com/wiselabaep/gmmnlse-solver-final>.
- [27] See Supplemental Material at <http://link.aps.org/supplemental/10.1103/PhysRevLett.126.093901> for full simulation and experimental details, which includes Refs. [28–33], and for videos showing the intracavity evolution of the pulse in the case of Fig. 1 (movie S1) and the intercavity evolutions of the pulse in the two cases of Fig. 4 (movie S2).
- [28] Z. Ziegler, Numerical tools for optical pulse propagation in multimode fiber, thesis, Cornell University, Ithaca, 2017.
- [29] A. Mahjoubfar, D. V. Churkin, S. Barland, N. Broderick, S. K. Turitsyn, and B. Jalali, Time stretch and its applications, *Nat. Photonics* **11**, 341 (2017).
- [30] X. Liu, X. Yao, and Y. Cui, Real-time observation of the buildup of soliton molecules, *Phys. Rev. Lett.* **121**, 023905 (2018).
- [31] K. Krupa, K. Nithyanandan, U. Andral, P. Tchofo-Dinda, and P. Grelu, Real-time observation of internal motion within ultrafast dissipative optical soliton molecules, *Phys. Rev. Lett.* **118**, 243901 (2017).
- [32] K. K. Cheung, C. Zhang, Y. Zhou, K. K. Wong, and K. K. Tsia, Manipulating supercontinuum generation by minute continuous wave, *Opt. Lett.* **36**, 160 (2011).
- [33] L. Gui, X. Xiao, and C. Yang, Observation of various bound solitons in a carbon-nanotube-based erbium fiber laser, *J. Opt. Soc. Am. B* **30**, 158 (2013).
- [34] H. Qin, X. Xiao, P. Wang, and C. Yang, Observation of soliton molecules in a spatiotemporal mode-locked multimode fiber laser, *Opt. Lett.* **43**, 1982 (2018).
- [35] Y. Ding, X. Xiao, P. Wang, and C. Yang, Multiple-soliton in spatiotemporal mode-locked multimode fiber lasers, *Opt. Express* **27**, 11435 (2019).
- [36] U. Teğin, E. Kakkava, B. Rahmani, D. Psaltis, and C. Moser, Spatiotemporal self-similar fiber laser, *Optica* **6**, 1412 (2019).
- [37] W. H. Renninger, A. Chong, and F. W. Wise, Pulse shaping and evolution in normal-dispersion mode-locked fiber lasers, *IEEE J. Sel. Topics Quantum Electron.* **18**, 389 (2011).
- [38] X. Feng, H.-y. Tam, and P. Wai, Stable and uniform multiwavelength erbium-doped fiber laser using nonlinear polarization rotation, *Opt. Express* **14**, 8205 (2006).
- [39] L. G. Wright, P. Sidorenko, H. Pourbeyram, Z. M. Ziegler, A. Isichenko, B. A. Malomed, C. R. Menyuk, D. N. Christodoulides, and F. W. Wise, Mechanisms of spatiotemporal mode-locking, *Nat. Phys.* **16**, 565 (2020).